Massive postglacial gene flow between European white oaks uncovered genes underlying species barriers

Thibault Leroy[1], **Quentin Rougemont**[2], **Jean-Luc Dupouey**[3], **Catherine Bodénès**[1], **Céline Lalanne**[1], **Caroline Belser**[4], **Karine Labadie**[4], **Grégoire Le Provost**[1], **Jean-Marc Aury**[4], **Antoine Kremer**[1,*], **Christophe Plomion**[1]

[1]BIOGECO, INRA, Univ. Bordeaux, 33610 Cestas, France

[2]Département de biologie, Institut de Biologie Intégrative et des Systèmes (IBIS), Université Laval, G1V 0A6, Québec, Canada

[3]INRA Université de Lorraine UMR 1137 'Ecologie et Ecophysiologie Forestières', route d'Amance, 54280 Champenoux, France

[4]CEA - Institut de Biologie François Jacob, Genoscope, 2 rue Gaston Crémieux, 91057 Evry, France

Abstract

• Oaks are dominant forest tree species widely distributed across the Northern Hemisphere, where they constitute natural resources of economic, ecological, social and historical value. Hybridization and adaptive introgression have long been thought to be major drivers of their ecological success. Thus, the maintenance of species barriers remains a key question, given the extent of interspecific gene flow.

• In this study, we made use of the tremendous genetic variation among four European white oak species (31 million SNPs) to infer the evolutionary history of these species, study patterns of genetic differentiation and identify reproductive barriers.

• We first analyzed the ecological and historical relationships among these species and inferred a long-term strict isolation followed by a recent and extensive postglacial contact using Approximate Bayesian Computation. Assuming this demographic scenario, we then performed backward simulations to generate the expected distributions of differentiation under neutrality to scan their genomes for reproductive barriers. We finally identified important intrinsic and ecological functions driving the reproductive isolation.

- We discussed the importance of identifying the genetic basis for the ecological preferences between these oak species and its implications for the renewal of European forests under global warming.

Keywords

Demographic inferences; reproductive isolation; speciation; intrinsic and ecological barriers; Genome scan; approximate Bayesian computation

Introduction

Oaks are a diverse group of about 350 to 500 species widely distributed throughout the Northern Hemisphere (Hubert *et al.*, 2014; Denk *et al.*, 2017). The variability in the number of recorded oak species highlights the challenge of delineating species limits within a genus displaying a high degree of morphological diversity, sometimes described as a "botanic horror" by taxonomists (Darwin, 1859; Palmer, 1948; Rieseberg *et al.*, 2006; Leroy *et al.*, 2019a). Genetic markers have corroborated these taxonomic concerns, particularly in European white oaks, which have been the subject of a large number of genetic surveys. Studies based on nuclear DNA markers have reported unambiguously high levels of admixture between European white oak species, confirming the reported taxonomic issues for oaks (Lepais *et al.*, 2009). Several detailed empirical studies based on chloroplast DNA markers have revealed an absence of private chlorotypes between European white oak species, but congruent associations between chlorotypes and expansion routes during the last postglacial recolonization, suggesting cytoplasmic capture via recurrent hybridization and backcrossing (Petit *et al.*, 1997; 2002). Recent advances in oak genomics (Plomion *et al.*, 2016; 2018) have made it possible to investigate interspecific gene flow at the whole-genome scale. Thus, Leroy *et al.* (2017) have provided evidence suggesting that extensive secondary contacts have occurred between four European white oak species, probably at the start of the current interglacial period. These results reconcile earlier findings of contrasting species differentiation at the nuclear and organelle levels. Indeed, secondary contacts explain present-day patterns of species differentiation, including complete sharing of haplotypes in mixed oak stands (Petit *et al.,* 2002) and the partial maintenance of nuclear genetic divergence at some loci (*e.g.* Scotti-Saintagne *et al.,* 2004). The inferences drawn are also consistent with the persistence of genomic regions impermeable to gene flow due to reproductive barriers, corresponding to a typical case of semi-isolated species (Leroy *et al.*, 2017). However, the genetic basis of these barriers remains unknown.

Controlled pollination trials have provided empirical evidence for the existence of strong reproductive barriers in these four European white oak species (Abadie *et al.*, 2012; Lepais *et al.*, 2013). Ecological preferences *in situ* have also been previously reported, with tolerance to dry (*Q. petraea*) or wet (*Q. robur*) sites (Eaton *et al.*, 2016), or acidic (*Q. pyrenaica*) or limy (*Q. pubescens*) soils (Timbal & Aussenal, 1996) but fine-grained ecological surveys do not yet exist for all these four species. The four species occupy different geographic ranges (Fig. 1A): extending up to Scandinavia for *Q. petraea* and *Q. robur*, whereas the other two species are present mostly in Mediterranean and sub-Mediterranean regions. However, the distribution ranges of these species overlap in some

areas, mostly in South-West France, but the four species are rarely found together in the same stand (but see Lepais *et al.*, 2009). The overlapping species ranges in South-West France thus provide an ideal "natural laboratory" (Hewitt, 1988) for investigating reproductive barriers between these European white oak species.

Here we combined state-of-the-art methods in population genomics to explore the genomic patterns of species differentiation (Fig. 2): (i) we used approximate Bayesian computation (ABC) to perform ascertainment bias-free demographic inferences in order to refine estimates of the timing of secondary contacts, and (ii) scan genomes for reproductive barriers. Our findings identified important intrinsic and ecological functions driving the reproductive isolation of these four oak species including tolerance to biotic and abiotic constraints, and intrinsic mating barriers.

Materials & Methods

Ecological niche of the four species

French data—We delineated the extant ecological niche of the four oak species in France (Figs. 1B, S1 and S2) by using their distribution maps based on the National Forest Inventory (Fig. S3) and climatic data extracted from the Chelsa data base (Karger *et al.*, 2017). In addition to the climatic data we added pH values of the soil. Proxies of pH values were derived from National Forest inventory floristic plots installed since 2005. Floristic composition of these inventory plots was compared to existing database (comprising floristic and physical data) to calculate proxies of pH values (Gégout *et al.*, 2005). We intersected the distribution maps with the climatic rasters (30" resolution) and using the R package "ggplot2" v. 2.2.1 (Wickham, 2009) calculated a 2D density plot of species presence in the ecological space as defined by climate (mean temperature) and soil pH.

European data—European distributions maps were constructed based on presence data of species made available by the European Forest Genetic Resources Programme (EUFORGEN, for *Q. robur* and *Q. petraea*, de Vries *et al.*, 2015) and the European atlas of forest tree species (JCR, San-Miguel-Ayanz *et al.*, 2016, for *Q. pyrenaica* & *Q. pubescens*). Climatic data are based on the Chelsa database (Karger *et al.*, 2017) and soil pH were derived from the European atlas of forest tree species data (JCR, San-Miguel-Ayanz *et al.*, 2016). Since these data were collected from different sites, we computed univariate (rather than bivariate) density distributions using ggplot2, using a procedure similar to that used for the French data.

Sampling and sequencing

We sampled populations of the four *Quercus* species in stands of natural origin located in South-West France. We sampled 13 *Q. petraea* trees from Laveyron (Landes, France), and 20 *Q. robur* and 20 *Q. pyrenaica* trees from the Landes EVOLTREE "Intensive Study Site" (ISS), 18 *Q. pubescens* trees from two sites in Gironde: 12 in Branne and 6 in Blaignan (Gironde, France) (see Table S1 for details). Samples of reference species populations came from the same geographic region. Such sampling strategy does not bias species comparison,

as shown by an earlier methodological study showing that species differentiation is only moderately impacted by the geographical origin of populations (Bodénès et al. 1997).

DNA was extracted from individual trees with the Invisorb Spin Plant Mini kit, according to the manufacturer's specification (Startec Molecular, GmbH, Berlin, Germany). DNA yields were evaluated with a NanoDrop 1000 spectrophotometer (NanoDrop Technologies, Wilmington, DE, USA) and DNA samples were mixed in equimolar amounts to obtain a single pool for each species.

In this study, we sequenced libraries of pooled DNA samples. Such a pool-seq approach is indeed a cost-and time-effective alternative to individual- sequencing. The main advantages include the reduction in the total sequencing effort and the costs for the preparation of the genomic libraries (e.g. Gautier *et al.,* 2013; Schlötterer *et al.,* 2014). If pool-seq data is expected to generate efficient allele frequency estimates under various experimental designs (Gautier *et al.,* 2013), a pool-seq strategy has also some limitations, especially the difficulty to reconstruct haplotype blocks and estimate linkage disequilibrium, at least for short reads, as used in this study. To meet the requirement of independence in some analyses (see the ABC section below), we randomly selected a low proportion of SNPs (one SNP every 15 Kb, on average), a far larger physical distance than the level of linkage disequilibrium generally assumed for oaks (*e.g.* <500 bp for the *Q. mongolica* var. *crispula* oak, Kremer *et al.,* 2012). For each pool, a paired-end DNA genomic library was generated with the Paired-End DNA Sample Preparation Kit (Illumina, San Diego, CA, USA). The library was then sequenced on a HiSeq2000 sequencer (Illumina, San Diego, CA, USA) with 2x100 paired-end reads. For each pool, we used nine to ten sequencing lanes.

Raw reads were trimmed to remove low-quality bases (<20) from the ends, and sequences between the second unknown nucleotide and the end of the reads were removed. Reads less than 30 nucleotides long after trimming were discarded.

Overall, between 1,617,465,418 and 1,813,403,677 reads per pool were retained for analysis, corresponding to 313 Gb (425X) to 356 Gb (483X) of raw data. Raw data have been deposited in the Sequence Read Archive (SRA): PRJEB23847.

Mapping and calling

All reads were then mapped against the v2.3 oak haplome assembly (Plomion et al., 2018), with bowtie2 v. 2.1.0 (Langmead & Salzberg, 2012), using standard parameters for the "sensitive end-to-end" mode. PCR duplicates were removed with Picard v. 1.106 (http://broadinstitute.github.io/picard/). Samtools v.1.1 (Li *et al.*, 2009) and Popoolation2 v. 1.201 (Kofler *et al.*, 2011) were then used to call biallelic SNPs with at least 10 copies of the alternate allele and a depth between 50 and 2000X at each position. To ensure a reasonably low rate of false positives due to Illumina sequencing errors, all SNPs with a MAF lower than 0.02 were discarded. We obtained allele counts for a total of 31,894,340 SNPs. F_{ST} in non-overlapping sliding-window was calculated from allele frequencies with the popoolation2 bioinformatics software suite (Kofler *et al.*, 2011).

Approximate Bayesian computation (ABC) analysis

Observed dataset—For all subsequent ABC analyses, we randomly selected 50,088 of the 31 million SNPs. For each of these SNPs, we multiplied allele frequencies by the number of set of chromosomes in each pool (26 for *Q. petraea*, 36 for *Q. pubescens* and 40 for both *Q. pyrenaica* and *Q. robur*) to generate the corresponding number of a specific allele in each pool. At this stage, we assumed that any departure from equimolarity due to bias in the mixing of DNA samples would have a negligible effect on our summary statistics calculated for a set of 50 thousand SNPs. Seventeen summary statistics were computed by *mscalc:* 1) the number of polymorphic sites specific to each gene pool, 2) the number of polymorphic sites existing in both gene pools, 3) nucleotide diversity (π) for each gene pool and, between gene pools, the mean value and standard variation for 4) gross divergence (Dxy), 5) net divergence (Da), 6) F_{ST}, and 7) Pearson's R^2 correlation coefficient in pi (see also Leroy *et al.*, 2017; Roux *et al.*, 2013; 2016). Demographic inferences based on summary statistics of the site frequency spectrum (SFS) are known to be robust to many sources of variation including the number of individuals and loci (Fraïsse *et al.* 2018). Besides, SFS-based inferences from pool-seq data have been shown to be robust (Christe *et al.* 2017).

Demographic scenarios—We used an ABC procedure similar to that described by Leroy and coworkers (2017). Briefly, we compared two different scenarios: isolation-with-migration (IM) and secondary contact (SC). Both scenarios assumed the subdivision of an ancestral panmictic population (PopAnc) into two daughter populations (Pop1 & Pop2) at time T_{SPLIT}, with population sizes remaining constant over time (N_{PopAnc}, N_{Pop1}, N_{Pop2}). The IM model assumed uninterrupted gene flow since T_{SPLIT}. The SC model assumed that populations initially evolved in strict isolation, with secondary gene flow beginning at some time before the present (at time T_{SC}, Leroy *et al.*, 2017).

Coalescent simulations—For coalescent simulations, we adapted the pipeline described by Leroy *et al.* (2017) for the calculation of summary statistics to large datasets (up to 100,000 SNPs). This pipeline includes a modified version of the random prior generator *priorgen* (Leroy *et al.*, 2017; Roux *et al.*, 2013; 2016), and the *msnsam* (Hudson, 2002; Ross-Ibarra *et al.*, 2008) and *mscalc* (Ross-Ibarra *et al.*, 2008; Roux *et al.*, 2016) programs. For each of the two scenarios (IM and SC), 1,000,000 random multilocus simulations were performed. Both models made use of genomic heterogeneity in effective migration rates (M) and population sizes (N_e) to take into account the occurrence of genomic barriers to gene flow and the confounding effect of linked selection. For both sources of heterogeneity, we used the strategy described by Leroy *et al.* (2017).

Model selection—The 500 best replicate simulations closest to the observed values were selected, and the posterior probabilities for each of the two scenarios (IM or SC) were estimated with a feed-forward neural network, by nonlinear multilocus regression (Leroy *et al.*, 2017 for details). ABC computations were performed with 20 feed-forward trained neural and 8 hidden networks.

Parameter estimation—Posterior distributions of the parameters were estimated with a two-step hierarchical procedure. We first evaluated the parameters under the best model, to check the consistency of our estimates, particularly concerning our previous support for very recent secondary contacts (Leroy *et al.*, 2017). We then ran an additional set of 1,000,000 coalescent simulations under an SC model, assuming that T_{SC} occurred in the last 5% of the divergence time, using a modified version of *priorgen*. This strategy was used to obtain more precise parameter estimates. For both rounds of estimation, we used a logit transformation of the parameters on the 500 best simulations providing the smallest Euclidean distance. The posterior probability of parameters was then estimated by the neural network procedure, from the means of weighted nonlinear multivariate regressions of the parameters on the summary statistics for 25 feed-forward trained neural and 10 hidden networks.

Genome scans

Coalescent simulations for outlier detection—For each pair of species, we ran 5,000,000 coalescent simulations, using parameter values sampled from the 95% confidence interval (CI) of the posterior distribution of all parameters for the pair considered. The simulations assumed genomic homogeneity for effective migration rates (M1 & M2) but heterogeneity for population size. Random values were generated with a modified version of *priorgen*. For each simulated locus, we then calculated He and G_{ST} with a custom-developed script. All scripts and datasets are publicly available for download from a GitHub repository (https://github.com/ThibaultLeroyFr/GenomeScansByABC). Extreme quantiles of the distribution of G_{ST} (99.99% of simulated values) relative to the expected heterozygosity of the locus were then calculated, with a strategy similar to that used for Fdist (Beaumont & Nichols, 1996). More specifically, a null envelope was computed from G_{ST} quantiles, with heterozygosity intervals of 2%. This strategy has the advantage of providing a null distribution of G_{ST} under much more complex scenarios (*i.e.* the best inferred demographic scenario) than other state-of-the art genome-scan methods.

For each of the 31 million SNPs, we computed the same summary statistics as for simulated neutral markers. The observed G_{ST} values conditioned by heterozygosity at the locus were compared to the previously generated null envelope. Markers with a G_{ST} value above this envelope were considered to be outliers. We then used a non-overlapping sliding-windows approach to estimate the proportion of outliers per 10-kb window. Windows containing fewer than 10 SNPs were discarded.

We generated parameter estimates under the best-fitting secondary contact model for each pair of species. Taking into account the 95% confidence intervals for each T_{SC}/T_{SPLIT} ratio (Tables 1 & S2) and the divergence time between these species (1-10 million years (Hubert *et al.*, 2014; Hipp *et al.*, 2018), the analysis yielded quite large estimates with secondary contact occurring between 100 and 62,400 years ago, corresponding to up to 1,225 generations, assuming a generation time of 50 years (Gregorius *et al.*, 2007).

Functional annotations

For the 227 genes found within regions enriched in outliers or in close vicinity to these regions (5 kb on both sides to exclude border effects, see "candidate regions" in Fig. 2), we

conducted BlastP searches in both the SwissProt and nr protein databases. Only BlastP results with e-values lower than 10e-5 were considered for protein function annotation. After identification of the protein function by BlastP analyses, functional annotations were performed using extensive manual literature searches rather than using automatic approaches based on gene ontology (GO)-oriented methods to ensure high quality gene annotations. We also reported information from a previous identification of orthologous and paralogous genes in 16 plant species, including *Q. robur*, performed with OrthoMCL (Plomion *et al.*, 2018 for details).

Results

Ecological preferences of the four species

We intersected the distribution maps of the four species (Fig. S3) with climatic and soil data derived from a large-scale floristic survey in France. Bivariate density distributions (Fig. 1B) show clear patterns of ecological preferences among the four white oak species. As expected, the two so called temperate white oaks (*Q. petraea* and *Q. robur*) are more frequently observed under cooler climates than Mediterranean and sub-Mediterranean species (*Q. pubescens* and *Q. pyrenaica*). Mean annual temperatures of the areas occupied by the two latter species extend up to 20°c, while the two former species occupy much cooler climates (mean temperature below 15°C). pH of the soils segregates particularly *Q. pyrenaica* from *Q. pubescens*. The modal value of the former species is close to 5, while the mode of the latter is around 7. Although we could not combine climatic and soil data over the whole species' ranges, univariate density distributions for both climate (Fig. S1) and soil pH (Fig. S2) based on continental-scale data showed similar trends.

Divergence and post-glacial secondary contact between European white oaks

A total of 31,894,340 SNPs were identified after the filtering of variants with a low minor allele frequency (MAF<0.02) in population samples for the four species (*Q. petraea, Q. robur, Q. pubescens, Q. pyrenaica*), corresponding to one SNP every 23.2 bp, on average. We also used genome-wide data for a *Q. suber* accession described by Leroy *et al.* (2017) to root a phylogenetic tree and investigate relationships between species for 9,084,835 of the 31.9 million SNPs. The best maximum-likelihood tree suggested that *Q. robur* initially diverged from the ancestor of the other three species (Fig. 1C).

We then randomly selected 50,088 SNPs from the entire set of 31.9 million SNPs for ascertainment bias-free demographic ABC inference. We compared two models of divergence with gene flow (Fig. 2) for each of the six possible species pairs: an isolation-with-migration model assuming constant gene flow since the divergence time (T_{SPLIT}), and a model assuming secondary contact with gene flow starting at $T_{SC,}$ a time point after divergence ($T_{SC} < T_{SPLIT}$). For all pairs, we obtained strong statistical support for the secondary contact model (>98% posterior probability, Tables 1 & S3 & Fig. S4), consistent with our previous findings based on individual data for 3,524 SNPs (Leroy *et al.*, 2017).

Interspecific genetic differentiation—Based on F_{ST} values calculated over 10-kb genome segments, the genetic differentiation between species pairs differed considerably

between chromosomes (Fig. S5), and, more interestingly, between segments within chromosomes (Fig. 3)

First, with rare exceptions, the three most strongly differentiated species pairs, for all oak chromosomes, were *Q. robur/Q. pubescens*, *Q. robur/Q. petraea* and *Q. pyrenaica/Q. petraea*. Lower levels of differentiation were observed for *Q. pubescens/Q. pyrenaica* and *Q.pubescens/Q.petraea* (Fig. S5A). These results suggest that the phylogenetic history of these species shaped the genomic landscape of differentiation such that the ranking of pairs of species according to mean F_{ST} values is conserved over chromosomes. Conversely, regardless of the pair of species considered, the interchromosomal variation of mean F_{ST} values was considerable (Fig. S5B), with significantly higher mean F_{ST} values for chromosomes 2 and 6 and significantly lower values for chromosome 4. For all pairs of species, the relationship between mean F_{ST} and the rate of recombination was significant at the chromosome scale ($P < 0.05$; Fig. S6), for calculations based on the comparison of the genetic length of each of the 12 linkage groups (Bodénès *et al.*, 2016) and the physical size of the corresponding pseudo-chromosomes (Plomion *et al.*, 2018), thus suggesting that the chromosomal recombination rate is a good predictor of the mean chromosomal F_{ST}.

Second, genome-wide patterns of F_{ST} variation plotted over the entire genome with 10-kb sliding windows (Fig. 3) revealed a highly heterogeneous differentiation landscape, even for the pair of species displaying the lowest range of differentiation according to F_{ST} values (*Q. pubescens/Q. robur*). Indeed 10-kb F_{ST} estimates between *Q. pubescens* and *Q. robur* ranged from 0 to 0.765. For the pairs of species including *Q. petraea*, the values for the window corresponding to the highest level of differentiation were 0.998 for *Q. petraea/Q. pyrenaica*, 0.999 for *Q. petraea/Q. robur* and 1 for *Q. petraea/Q. pubescens*. On closer inspection, very narrow regions of very high F_{ST} were identified on several chromosomes, for most pairs of species (Fig. 3, chromosomes 1, 7, 9, and 11, for example).

Narrow regions of non-neutral evolution

We then took advantage of these demographic inferences to perform differentiation outlier tests. We performed extensive backward simulations (5,000,000 independent SNPs) under the best inferred scenario to generate null distributions for each pairwise comparison (Fig. S7, see also Notes S1). The most outlier-enriched windows were retained for the identification of candidate genes underlying species barriers (after excluding SNPs with very low heterozygosities, Figs. 2 & S8). We identified 281 windows containing the highest proportion of outliers (top 0.1% of window enriched in outliers for at least one pair of species). We then analyzed the clustering of these outlier-enriched windows. We defined a candidate genomic region by merging close windows, *e.g.* two contiguous sequences of two outlier-enriched windows, with possible interruption by a single undetected window (Fig. 2). The 281 windows were distributed over 215 candidate genomic regions, distributed over all chromosomes (blue lines, Fig. 4).

We listed all the *Quercus* genes located within or flanking these 215 genomic regions. We identified 227 genes distributed over 133 of the 215 regions, with very few candidates per region (mean: 1.71±1.76 genes per region, 1.49 ±0.82 genes after excluding 5 regions with chloroplast-like DNA signatures, see also Notes S2). On all these genes, we performed

extensive literature searches to generate manually curated gene annotations. Albeit non-exhaustive by definition, manual literature searches represent more than ever a relevant alternative to methods based on automatically extracted information from literature. Improving the accuracy and traceability of the gene annotations is especially important in oaks since genetic-engineering methods, such as forward and reverse genetic approaches, are not yet available for oaks and gene functions cannot be fully validated based on their phenotypic impacts.

In the following sections, we discuss three major functional categories on the basis of their known implications for ecological and intrinsic reproductive isolation (Dataset S1 for all information). These 3 functional categories contain at least 32 candidate genes (Table 2) among the 227 detected genes (Table S4 and Dataset S1 for details). The first category comprises genes underlying the ecological preferences of the four species: tolerance of water deficit, cold tolerance, adaptation to alkaline soils. The second includes genes involved in biotic interactions, such as immune responses, resistance to biotic stresses, and mycorrhization. The third gathers genes probably involved in intrinsic barriers, and includes genes with functions related to flowering time, pollen recognition, pollen growth and embryo development.

Species-specific ecological and non-ecological reproductive barriers

Unlike studies aiming at interpreting every region enriched in outliers, our objective was rather to focus on genes displaying distinct patterns among pairs of species. This is especially important since these patterns are unexpected to arise via background selection (see Notes S3 for details). After excluding genes with a "shared" pattern (see Table 2), several different cases were observed (Table S5): (i) 9 regions enriched in outliers for all but one pair of species (including 7 regions for all pairs except *Q. robur* – *Q. petraea* and 2 regions for all pairs except *Q. pubescens* – *Q. pyrenaica* pairs), (ii) 5 regions specific to all pairs sharing the same species (4 for *Q. pyrenaica* and 1 for *Q. pubescens*) and (iii) 11 regions with more complex patterns.

Among the nine regions with an "all-versus-one-pair" relationship, seven excluded the *Q. robur*/*Q. petraea* pair and the other two excluded the *Q. pubescens*/*Q. pyrenaica* pair. Four of the seven candidate genes for which a pattern "all except *Q. robur*/*Q. petraea* pair" was observed are known to be involved in drought tolerance or in lateral root growth (Table 2). This pattern is consistent with the higher drought tolerance of *Q. pyrenaica* and *Q. pubescens* compared to *Q. petraea* or *Q. robur* (Fonti *et al.*, 2013). Reciprocally, we observed an "all vs. one" pattern (undetected for the *Q. robur*-/*Q. petraea* pair) for a VRN1 gene involved in responsiveness to vernalization and known to play a key role in cold acclimation in many plant species (Levy *et al.*, 2002). Overall, the genomic variation of these nine genes parallels the Northern-Southern distribution of the studied species, suggesting that the underlying barriers are driven by climate preferences (Fig. 1 A, B).

Among the five candidate genes from genomic regions with branch-specific patterns, *i.e.* deviating from neutrality in all pairs containing a given species, four have *Q. pyrenaica*-specific patterns, including three encoding G-type lectin S-receptor-like serine/threonine kinases (LECRKs) and one encoding a transportin (MOS14). The former is known to be

essential for proper splicing of several resistance genes in *Arabidopsis* (Xu *et al.*, 2011), and therefore suggests substantial interspecific differences in plant immunity. Along with the four regions containing genes with *Q. pyrenaica* specific alleles, we identified a fifth-species-specific pattern *for Q. pubescens*. The gene encodes a metal transporter (Nramp5) involved in the assimilation of manganese and cadmium in rice and barley (Wu *et al.*, 2016).

Among genes with complex patterns, we identified many candidate genes for intrinsic premating and postmating barriers. We identified several genes involved in the timing of flowering, including APETALA2 and PRR73. APETALA2 is a key transcription factor for the establishment of the floral meristem (Irish & Sussex, 1990). Similarly, PRR73 contributes to flowering time variation in barley and wheat (Higgins *et al.*, 2010 and references therein).

Discussion

The increasing availability of genomic resources for phylogenetically related species has the potential to greatly improve our understanding of their evolutionary trajectories and the molecular basis of their reproductive isolation as shown here for European temperate oaks. Our demographic reconstruction supports long periods of isolation between these oak species for most of their history leading to the gradual loss of shared alleles and the accumulation of reproductive barriers.

Systematic shift in the evolutionary trajectories

We found evidence of a systematic shift in the evolutionary trajectories that occurred at the transition between the last glacial maximum and subsequent postglacial period. More precisely, this shift took place while the oak species were migrating northwards as the climate became warmer, and resulted in their encountering in central Europe. Even if the results reported here are in line with our previous findings (Leroy *et al.*, 2017), this study is based on ascertainment bias-free analyses and use of 10 times as many SNPs. The genome-wide investigation performed here provided stronger support for the occurrence of secondary contact. Indeed, the previous inferences were drawn from a dataset with a strong ascertainment bias. Such a deviation from the true site frequency spectrum is known to have a negative impact on the performance of likelihood-free analyses (Albrechtsen *et al.*, 2010). As in our previous report, our ABC inferences were found to be highly robust to alternative models based on 1000 pseudo-observed datasets, indicating that the probability of an incorrect inference of secondary contact was very low (Fig. S4).

In addition, our use of 10 times as many SNPs and a two-round procedure to generate parameter estimates made it possible to narrow down the time frame over which these contacts took place. After confirming that recent secondary contact had occurred between these four species, we ran additional backward simulations explicitly assuming recent secondary contact (Tsc < 5% Tsplit), to ensure high accuracy for parameter estimates. Assuming that T_{SPLIT} occurred between 1 and 5 million years ago (MYA) (Hubert *et al.*, 2014) or between 7 and 10 MYA (Denk *et al.*, 2017), and taking into account the 95% confidence intervals for each T_{SC}/T_{SPLIT} ratio (Table S2), we estimated that secondary contacts occurred between 100 and 62,400 years ago, corresponding to up to 1,225

generations, assuming a generation time of 50 years (Gregorius *et al.* 2007, but see also in this issue Leroy *et al.,* 2019a, for a discussion about the uncertainties with regard to the oak generation times), whereas the upper bound for our previous estimate was 11,200 generations (Leroy *et al.*, 2017). Overall, the median estimates of the timing of secondary contact ranged from 2,450 to 21,760 years depending on the species pair considered (49 to 435 generations), consistent with the general hypothesis of a resumption of secondary gene flow at the start of the current interglacial period.

In line with our previous conclusions (Leroy *et al.*, 2017), our inferences cannot however exclude that a few secondary contact periods had already taken place earlier. Since we did not allow for the possibility of multiple periods of contact and isolation in our model, it remains impossible to know if some (few) other periods of contacts had already taken place earlier during the divergence of these species. Indeed, we used summary statistics that are not expected to capture this information well enough in order to be conclusive. However, it should be noted that a scenario with lot of secondary contact periods (e.g. once every past postglacial period) remains unlikely, since it would have generated a much higher posterior probability for IM scenarios. In addition, historical variations in effective population sizes are not taken into account. Further work to infer evolutionary history of these species based on summary statistics at the gene scale (*ie* based on summary statistics accounting for linkage disequilibrium) rather than those at the base scale will likely have more power to capture these more complex scenarios. Lastly, our analyses are only based on pairwise comparisons. Joint inferences of the evolutionary history of the four (or more) European white oak species should provide additional information about the evolutionary history of these species, especially regarding the direction of interspecific gene flow.

Highly heterogeneous genetic differentiation landscape

The mixture of different species and populations in central Europe occurring during the Holocene was so massive that private (or near private alleles) were redistributed among these interfertile species. Indeed, current levels of interspecific differentiation are extremely low along almost all the genome (mean interchromosomal 10-kb estimates of F_{ST} below 0.08 for all pairs) confirming earlier reports by Scotti-Saintagne et al. (2004). Recently, Lang *et al.* (2018) reported a slightly higher mean F_{ST} value for the *Q. robur*/*Q. petraea* pair (mean F_{ST}=0.13 over ~12,500 SNPs) based on a restricted representation strategy, representing a total sequence data of ~530 Kb (0.072% of the oak genome, Plomion *et al.,* 2018). The differences need to be treated with caution because both estimates are potentially slightly biased. Indeed, we do not rule out the possibility that our estimate is negatively impacted by some DNA quantification and pipetting errors or some unfiltered sequencing errors (Gautier *et al.*, 2013; Hivert *et al.*, 2018). Reciprocally, Lang *et al.* (2018) targeted some genes potentially involved in species ecological preferences that may have resulted in an overestimation of the mean F_{ST} value. Notwithstanding the uncertainty in both estimates, these reported values are consistent with an overall low current level of differentiation and are at a level compatible with many reports of within-species population structure in the literature (Roux *et al.*, 2016).

Interestingly, chromosomal F_{ST} estimates differed considerably between pairs of species and chromosomes. For all pairs, inter-chromosomal F_{ST} variation was significantly correlated with variations of chromosomal recombination rate (Fig. S6). This is consistent with the increasing number of reports for a correlation between the recombination rate and the rates of introgression, e.g. in the house mouse (Janoušek *et al.*, 2015), in *Mimulus* monkey flowers (Aeschbacher *et al.*, 2017), in *Heliconius* butterflies (Martin *et al.*, 2019) or in humans (Juric *et al.*, 2016) and expected to be due to the variation of linkage to introgressed deleterious alleles (background selection, Charlesworth *et al.*, 1993). The recent report of a remarkably high rate of deleterious mutations relative to 28 other plant species (Plomion *et al.*, 2018) highlights the putative role of deleterious mutations in shaping the genomic landscape of species differentiation in oaks. The contribution of linkage to the genomic width of reproductive barriers appears to be limited, as no long stretches of extensive differentiation were observed. We identified very restricted, widely distributed "islands" of high differentiation. The high-resolution genetic landscape of differentiation observed with scattered microislands of high F_{ST} on otherwise poorly differentiated chromosomes contrasts sharply with many other F_{ST} scan studies reporting either continents of differentiation (e.g. Tine *et al.*, 2014) or islands of high differentiation in highly structured populations (e.g. Renaut *et al.*, 2013).

To summarize thus far, extensive secondary gene flow over the last 20,000 years, together with very high levels of prezygotic and postzygotic selection (Abadie *et al.*, 2012; Lepais *et al.*, 2013), probably eroded interspecific genetic structures other than those at barrier loci, thereby generating a highly heterogeneous differentiation landscape. At some narrow regions distributed throughout the genome, interspecific differentiation however reaches extremely high levels (10-kb estimates of F_{ST} above 0.8). These peaks most likely correspond to narrow regions where selection counteracted the homogenizing effect of gene flow, thus leading to the present-day highly heterogeneous landscape of differentiation.

Candidate genes for drought tolerance and insights for the renewal of oak forests—The highest differentiated SNPs contributing to reproductive barriers mostly set apart Southern (*Q. pyrenaica* & *Q. pubescens*) from Northern species (*Q. robur* & *Q. petraea*). While this observation is inconsistent with the inferred phylogeny (Fig. 1C and Leroy *et al.*, 2017), it however coincides with the climatic preferences of the four species (Fig. 1 A,B). Indeed, all genes with an "all-versus-one-pair" relationship parallel the Northern-Southern distribution of the studied species, suggesting that the underlying barriers are driven by ecological preferences. Given that dehydration-associated genes currently act as strong barriers between these species in South-West France, we question whether drought tolerance alleles from *Q. pubescens* and *Q. pyrenaica* would introgress easily into the *Q. petraea* or *Q. robur* genomes. In a companion paper (Leroy et al. 2019b), we found evidence for adaptive introgression from *Q. robur* to Q. petraea populations located at the northern and higher elevational margins. Such introgressed genes were enriched in alleles exhibiting higher *Q. petraea/Q.robur* differentiation. These results suggest that introgression may override species barriers between these four white oaks under peculiar ecological contexts, and potentially contribute to adaptation (e.g. Bontrager & Angert, 2019; Suarez-Gonzalez *et al.*, 2018; Taylor & Larson, 2019). As Mediterranean oak species (*Q. pyrenaica* & *Q.*

pubescens) are likely to migrate northwards due to climate change, we anticipate that opportunities for hybridization with temperate species (*Q. petraea - Q. robur*) may increase, leading potentially to introgression enhancing adaptation of the temperate species to warmer climates.

In addition, we found genetic support for *Q. pubescens* preference for alkaline soils and found evidence for one key gene, Nramp5. Indeed Nramp5 is involved in the assimilation of manganese and cadmium in rice and barley (Wu *et al.*, 2016). Manganese assimilation is known to be essential for many plant functions, but manganese availability in the soil tends to decrease with increasing pH, and becomes limiting beyond a soil pH of 6.5. This metal transporter gene probably indicates a greater ecological preference of *Q. pubescens* for dolomitic soils (Fig. 1B) in comparison to the other three species.

We also found differences between *Q. pyrenaica* and the three other species at genes involved in plant immunity, in line with previous reports for higher mortality rates in this species due to pathogens (Desprez-Loustau *et al.*, 2011 and references therein). Indeed, *Q. pyrenaica* is known to be extremely sensitive to oak powdery mildew, a pathogen that was introduced into Europe at the start of the 20th century. Soon after the first detection of the fungus in Europe, high mortality rates were reported for *Q. pyrenaica* in the humid warm-temperate forests of Southwestern and Western France (Desprez-Loustau *et al.*, 2011). *Q. pyrenaica*-specific alleles at these genes may be the signature of the high susceptibility of *Q. pyrenaica* to biotic stresses in moist environments. It however remains to be studied why these genes act as reproductive barriers.

In addition, we identified several candidate genes for intrinsic barriers likely involved in pollen or embryo development, suggesting that both premating and postmating intrinsic barriers operate in oaks as suggested by Bodénès et al. (2016). Three of these genes encode cycloartenol synthases known to be essential for pollen development in *Arabidopsis* (Badiychuk *et al.*, 2008). Interestingly, some genes can have pleiotropic effects, that may act at both ecological and mating levels. *VRN1* is a case of point. In addition to its primary role in vernalization, VRN1 is involved in the repression of *FLC* (itself a known repressor of flowering) in *Arabidopsis,* through a vernalization-independent floral pathway (Levy *et al.*, 2002).

Overall, our results suggest that key selective abiotic and biotic factors triggered by post glacial environmental changes have molded the extant landscape of species reproductive barriers in European temperate oak species. We anticipate that these drivers will operate during ongoing climate changes as Mediterranean oak species (*Q. pyrenaica* & *Q. pubescens*) are migrating northwards getting in contact in more Northern latitudes with local temperate species (*Q. petraea* and *Q. robur*).

Supplementary Material

Refer to Web version on PubMed Central for supplementary material.

Acknowledgments

References

Abadie P, Roussel G, Dencausse B, Bonnet C, Bertocchi E, Louvet J-M, Kremer A, Garnier-Géré P. Strength, diversity and plasticity of postmating reproductive barriers between two hybridizing oak species (*Quercus robur* L. and *Quercus petraea* (Matt) Liebl.). Journal of Evolutionary Biology. 2012; 25:157–173. [PubMed: 22092648]

Aeschbacher S, Selby JP, Willis JH, Coop G. Population-genomic inference of the strength and timing of selection against gene flow. Proceedings of the National Academy of Sciences. 2017; 114:7061.

Albrechtsen A, Nielsen FC, Nielsen R. Ascertainment Biases in SNP Chips Affect Measures of Population Divergence. Molecular Biology and Evolution. 2010; 27:2534–2547. [PubMed: 20558595]

Babiychuk E, Bouvier-Navé P, Compagnon V, Suzuki M, Muranaka T, Van Montagu M, Kushnir S, Schaller H. Allelic mutant series reveal distinct functions for *Arabidopsis* cycloartenol synthase 1 in cell viability and plastid biogenesis. Proceedings of the National Academy of Sciences. 2008; 105:3163.

Beaumont MA, Nichols RA. Evaluating loci for use in the genetic analysis of population structure. Proceedings of the Royal Society of London Series B: Biological Sciences. 1996; 263:1619–1626.

Bodénès C, Chancerel E, Ehrenmann F, Kremer A, Plomion C. High-density linkage mapping and distribution of segregation distortion regions in the oak genome. DNA Res. 2016; 23:115–124. [PubMed: 27013549]

Bodénès C, Joandet S, Laigret F, Kremer A. Detection of genomic regions differentiating two closely related oak species *Quercus petraea* (Matt.) Liebl. and *Quercus robur* L. Heredity. 1997; 78:433–444.

Bontrager M, Angert AL. Gene flow improves fitness at a range edge under climate change. Evolution letters. 2018; 3:55–68. [PubMed: 30788142]

Charlesworth B, Morgan MT, Charlesworth D. The effect of deleterious mutations on neutral molecular variation. Genetics. 1993; 134:1289. [PubMed: 8375663]

Christe C, Stölting KN, Paris M, Fraïsse C, Bierne N, Lexer C. Adaptive evolution and segregating load contribute to the genomic landscape of divergence in two tree species connected by episodic gene flow. Molecular Ecology. 2017; 26:59–76. [PubMed: 27447453]

Darwin, C. On the Origin of Species by Means of Natural Selection: Or the Preservation of Favoured Races in the Struggle for Life. (5th edition). London, UK: John Murray; 1869.

Denk T, Grimm GW, Manos PS, Deng M, Hipp AL. An updated infrageneric classification of the oaks: review of previous taxonomic schemes and synthesis of evolutionary patterns. bioRxiv. 2017; doi: 10.1101/168146

Desprez-Loustau M-L, Feau N, Mougou-Hamdane A, Dutech C. Interspecific and intraspecific diversity in oak powdery mildews in Europe: coevolution history and adaptation to their hosts. Mycoscience. 2011; 52:165–173.

Eaton, E, Caudullo, G, Oliveira, S, de Rigo, D. *Quercus robur* and *Quercus petraea* in Europe: distribution, habitat, usage and threatsEuropean Atlas of Forest Tree Species. San-Miguel-Ayanz, J, de Rigo, D, Caudullo, G, Houston Durrant, T, Mauri, A, editors. Luxembourg City, Luxembourg: The publications office of the European Union; 2016. European Atlas of Forest Tree Species. pp. e01c6df+

Fonti P, Heller O, Cherubini P, Rigling A, Arend M. Wood anatomical responses of oak saplings exposed to air warming and soil drought. Plant Biology. 2013; 15:210–219.

Fraïsse C, Roux C, Gagnaire P-A, Romiguier J, Faivre N, Welch JJ, Bierne N. The divergence history of European blue mussel species reconstructed from Approximate Bayesian Computation: the effects of sequencing techniques and sampling strategies. PeerJ. 2018; 6:e5198. [PubMed: 30083438]

Gautier M, Foucaud J, Gharbi K, Cézard T, Galan M, Loiseau A, Thomson M, Pudlo P, Kerdelhué C, Estoup A. Estimation of population allele frequencies from next-generation sequencing data: pool-versus individual-based genotyping. Molecular Ecology. 2013; 22:3766–3779. [PubMed: 23730833]

Gégout JC, Coudun C, Bailly G, Jabiol B. EcoPlant: A forest site database linking floristic data with soil and climate variables. Journal of Vegetation Science. 2005; 16:257–260.

Gregorius HR, Degen B, König A. Problems in the Analysis of Genetic Differentiation Among Populations – a Case Study in *Quercus robur*. Silvae Genetica. 2007; 56:190–199.

Hewitt GM. Hybrid zones-natural laboratories for evolutionary studies. Trends in Ecology & Evolution. 1988; 3:158–167. [PubMed: 21227192]

Higgins JA, Bailey PC, Laurie DA. Comparative Genomics of Flowering Time Pathways Using *Brachypodium distachyon* as a Model for the Temperate Grasses. PLOS ONE. 2010; 5:e10065. [PubMed: 20419097]

Hipp AL, Manos PS, González-Rodríguez A, Hahn M, Kaproth M, McVay JD, Avalos SV, Cavender-Bares J. Sympatric parallel diversification of major oak clades in the Americas and the origins of Mexican species diversity. New Phytologist. 2018; 217:439–452. [PubMed: 28921530]

Hivert V, Leblois R, Petit EJ, Gautier M, Vitalis R. Measuring Genetic Differentiation from Pool-seq Data. Genetics. 2018; 210:315. [PubMed: 30061425]

Gregorius HR, Degen B, König A. Problems in the Analysis of Genetic Differentiation Among Populations – a Case Study in *Quercus robur*. Silvae Genetica. 2007; 56:190–199.

Hubert F, Grimm GW, Jousselin E, Berry V, Franc A, Kremer A. Multiple nuclear genes stabilize the phylogenetic backbone of the genus *Quercus*. Systematics and Biodiversity. 2014; 12:405–423.

Hudson RR. Generating samples under a Wright–Fisher neutral model of genetic variation. Bioinformatics. 2002; 18:337–338. [PubMed: 11847089]

Irish VF, Sussex IM. Function of the apetala-1 gene during Arabidopsis floral development. The Plant Cell. 1990; 2:741. [PubMed: 1983792]

Janoušek V, Munclinger P, Wang L, Teeter KC, Tucker PK. Functional organization of the genome may shape the species boundary in the house mouse. Molecular biology and evolution. 2015; 32:1208–1220. [PubMed: 25631927]

Gégout JC, Coudun C, Bailly G, Jabiol B. EcoPlant: A forest site database linking floristic data with soil and climate variables. Journal of Vegetation Science. 2005; 16:257–260.

Juric I, Aeschbacher S, Coop G. The Strength of Selection against Neanderthal Introgression. PLOS Genetics. 2016; 12:e1006340. [PubMed: 27824859]

Karger DN, Conrad O, Böhner J, Kawohl T, Kreft H, Soria-Auza RW, Zimmermann NE, Linder HP, Kessler M. Climatologies at high resolution for the earth's land surface areas. Scientific Data. 2017; 4

Kremer A, Abbott AG, Carlson JE, Manos PS, Plomion C, Sisco P, Staton ME, Ueno S, Vendramin GG. Genomics of Fagaceae. Tree Genetics & Genomes. 2012; 8:583–610.

Kofler R, Pandey RV, Schlötterer C. PoPoolation2: identifying differentiation between populations using sequencing of pooled DNA samples (Pool-Seq). Bioinformatics. 2011; 27:3435–3436. [PubMed: 22025480]

Lang T, Abadie P, Léger V, Decourcelle T, Frigerio J-M, Burban C, Bodénès C, Guichoux E, Le Provost G, Robin C, et al. High-quality SNPs from genic regions highlight introgression patterns among European white oaks (*Quercus petraea* and *Q. robur*). bioRxiv. 2018; doi: 10.1101/388447

Langmead B, Salzberg SL. Fast gapped-read alignment with Bowtie 2. Nature Methods. 2012; 9:357–359. [PubMed: 22388286]

Lepais O, Petit RJ, Guichoux E, Lavabre JE, Alberto F, Kremer A, Gerber S. Species relative abundance and direction of introgression in oaks. Molecular Ecology. 2009; 18:2228–2242. [PubMed: 19302359]

Lepais O, Roussel G, Hubert F, Kremer A, Gerber S. Strength and variability of postmating reproductive isolating barriers between four European white oak species. Tree Genetics & Genomes. 2013; 9:841–853.

Leroy T, Kremer A, Plomion C. Oak symbolism in the light of genomics. New Phytologist. 2019a; doi: 10.1111/nph.15987

Leroy T, Louvet J-M, Lalanne C, Le Provost G, Labadie K, Aury J-M, Delzon S, Plomion C, Kremer A. Adaptive introgression as driver of local adaptation to climate in European white oaks. bioRxiv. 2019b; doi: 10.1101/584847

Leroy T, Roux C, Villate L, Bodénès C, Romiguier J, Paiva JAP, Dossat C, Aury J-M, Plomion C, Kremer A. Extensive recent secondary contacts between four European white oak species. New Phytologist. 2017; 214:865–878. [PubMed: 28085203]

Levy YY, Mesnage S, Mylne JS, Gendall AR, Dean C. Multiple Roles of Arabidopsis VRN1 in Vernalization and Flowering Time Control. Science. 2002; 297:243. [PubMed: 12114624]

Li H, Handsaker B, Wysoker A, Fennell T, Ruan J, Homer N, Marth G, Abecasis G, Durbin R, 1000 Genome Project Data Processing Subgroup. The Sequence Alignment/Map format and SAMtools. Bioinformatics. 2009; 25:2078–2079. [PubMed: 19505943]

Martin SH, Davey JW, Salazar C, Jiggins CD. Recombination rate variation shapes barriers to introgression across butterfly genomes. PLOS Biology. 2019; 17:e2006288. [PubMed: 30730876]

Palmer EJ. HYBRID OAKS OF NORTH AMERICA. Journal of the Arnold Arboretum. 1948; 29:1–48.

Petit RJ, Csaikl UM, Bordács S, Burg K, Coart E, Cottrell J, van Dam B, Deans JD, Dumolin-Lapègue S, Fineschi S, et al. Chloroplast DNA variation in European white oaks: Phylogeography and patterns of diversity based on data from over 2600 populations. Range wide distribution of chloroplast DNA diversity and pollen deposits in European white oaks: inferences about colonisation routes and management of oak genetic resources. Forest Ecology and Management. 2002; 156:5–26.

Petit RJ, Pineau E, Demesure B, Bacilieri R, Ducousso A, Kremer A. Chloroplast DNA footprints of postglacial recolonization by oaks. Proceedings of the National Academy of Sciences. 1997; 94:9996–10001.

Plomion C, Aury J-M, Amselem J, Alaeitabar T, Barbe V, Belser C, Bergès H, Bodénès C, Boudet N, Boury C, et al. Decoding the oak genome: public release of sequence data, assembly, annotation and publication strategies. Molecular Ecology Resources. 2016; 16:254–265. [PubMed: 25944057]

Plomion C, Aury J-M, Amselem J, Leroy T, Murat F, Duplessis S, Faye S, Francillonne N, Labadie K, Le Provost G, et al. Oak genome reveals facets of long lifespan. Nature Plants. 2018; 4:440–452. [PubMed: 29915331]

Renaut S, Grassa CJ, Yeaman S, Moyers BT, Lai Z, Kane NC, Bowers JE, Burke JM, Rieseberg LH. Genomic islands of divergence are not affected by geography of speciation in sunflowers. Nature Communications. 2013; 4:1827.

Rieseberg LH, Wood TE, Baack EJ. The nature of plant species. Nature. 2006; 440:524–527. [PubMed: 16554818]

Ross-Ibarra J, Wright SI, Foxe JP, Kawabe A, DeRose-Wilson L, Gos G, Charlesworth D, Gaut BS. Patterns of Polymorphism and Demographic History in Natural Populations of *Arabidopsis lyrata*. PLoS ONE. 2008; 3:e2411. [PubMed: 18545707]

Roux C, Fraïsse C, Romiguier J, Anciaux Y, Galtier N, Bierne N. Shedding Light on the Grey Zone of Speciation along a Continuum of Genomic Divergence. PLOS Biology. 2016; 14:e2000234. [PubMed: 28027292]

Roux C, Tsagkogeorga G, Bierne N, Galtier N. Crossing the species barrier: genomic hotspots of introgression between two highly divergent *Ciona intestinalis* species. Molecular Biology and Evolution. 2013; 30:1574–1587. [PubMed: 23564941]

San-Miguel-Ayanz, J, de Rigo, D, Caudullo, G, Houston Durrant, T, Mauri, A, Tinner, W, Ballian, D, Beck, P, Birks, H, Eaton, E. , et al. European atlas of forest tree species. Luxembourg City, Luxembourg: The publications office of the European Union; 2016.

Schlötterer C, Tobler R, Kofler R, Nolte V. Sequencing pools of individuals — mining genome-wide polymorphism data without big funding. Nature Reviews Genetics. 2014; 15:749.

Scotti-Saintagne C, Mariette S, Porth I, Goicoechea PG, Barreneche T, Bodénès C, Burg K, Kremer A. Genome Scanning for Interspecific Differentiation Between Two Closely Related Oak Species [*Quercus robur* L. and *Q. petraea* (Matt.) Liebl.]. Genetics. 2004; 168:1615. [PubMed: 15579711]

Suarez-Gonzalez A, Lexer C, Cronk QCB. Adaptive introgression: a plant perspective. Biology letters. 2018; 14

Taylor SA, Larson EL. Insights from genomes into the evolutionary importance and prevalence of hybridization in nature. Nature Ecology & Evolution. 2019; 3:170–177. [PubMed: 30697003]

Timbal J, Aussenac G. An overview of ecology and silviculture of indigenous oaks in France. Annals of Forest Science. 1996; 53:649–661.

Tine M, Kuhl H, Gagnaire P-A, Louro B, Desmarais E, Martins RST, Hecht J, Knaust F, Belkhir K, Klages S, et al. European sea bass genome and its variation provide insights into adaptation to euryhalinity and speciation. Nature Communications. 2014; 5:5770.

de Vries, S, Murat, A, Bozzano, M, Burianek, V, Collin, E, Cottrell, J, Ivankovic, M, Kelleher, C, Koskela, J, Rotach, P. , et al. Pan-European strategy for genetic conservation of forest trees and establishment of a core network of dynamic conservation units. Rome, Italy: Bioversity International; 2015. 40

Wickham, H. ggplot2: Elegant Graphics for Data Analysis. Springer-Verlag; New York: 2016.

Wu D, Yamaji N, Yamane M, Kashino-Fujii M, Sato K, Feng Ma J. The HvNramp5 Transporter Mediates Uptake of Cadmium and Manganese, But Not Iron. Plant Physiology. 2016; 172:1899. [PubMed: 27621428]

Xu S, Zhang Z, Jing B, Gannon P, Ding J, Xu F, Li X, Zhang Y. Transportin-SR Is Required for Proper Splicing of Resistance Genes and Plant Immunity. PLOS Genetics. 2011; 7:e1002159. [PubMed: 21738492]
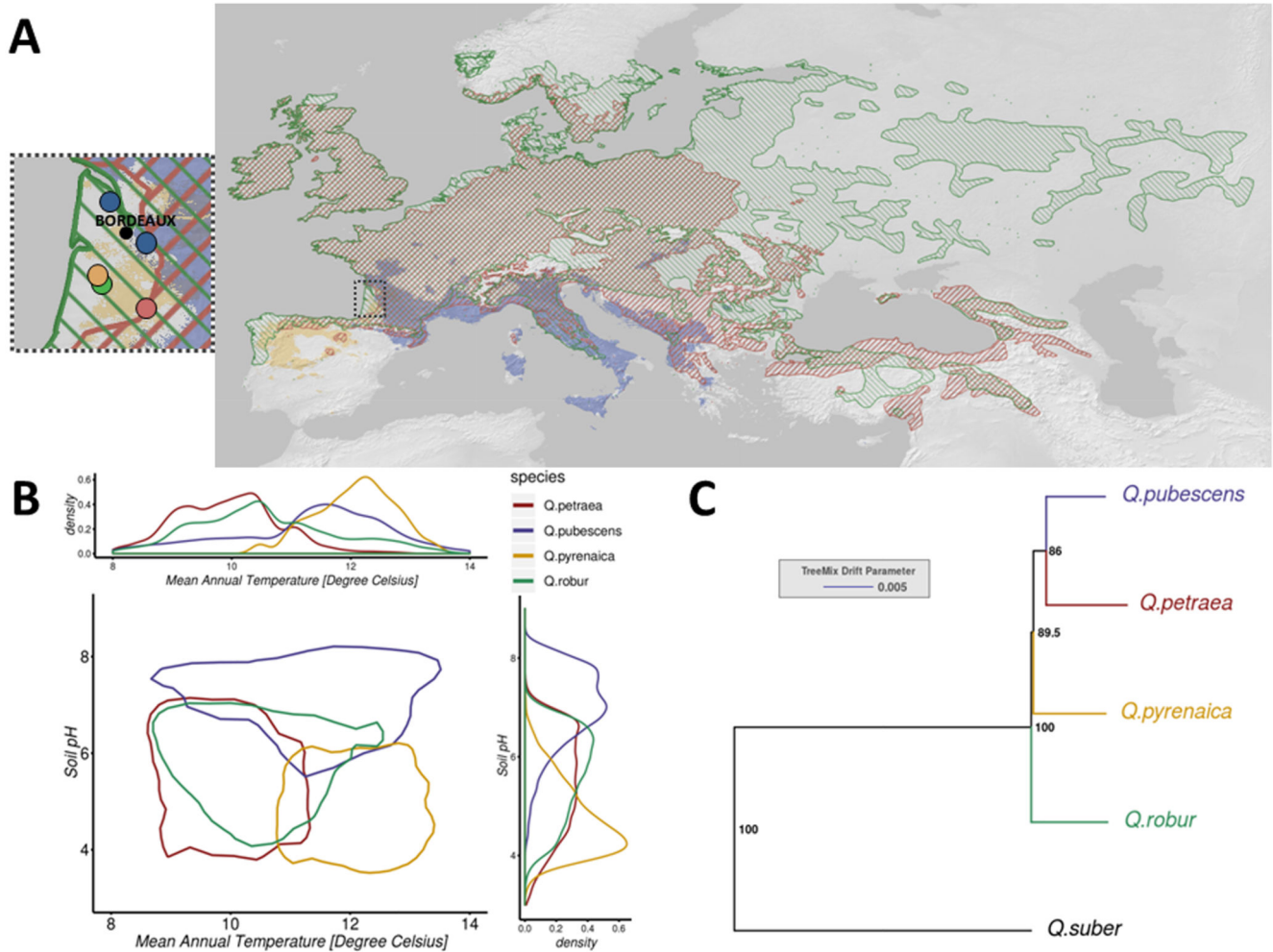
Fig. 1. Continental-scale species distributions and origin of the study material (A) and, ecological (B) and phylogenic relationships of the four European white oak species under investigation using TreeMix (C).

B) The central plot shows the contour of the two-dimensional density between the soil pH and the mean annual temperature enclosing 95% of the ecological data values, based on the French data only. The above and right charts show the one-dimensional density curves for mean annual temperature and soil pH, respectively.
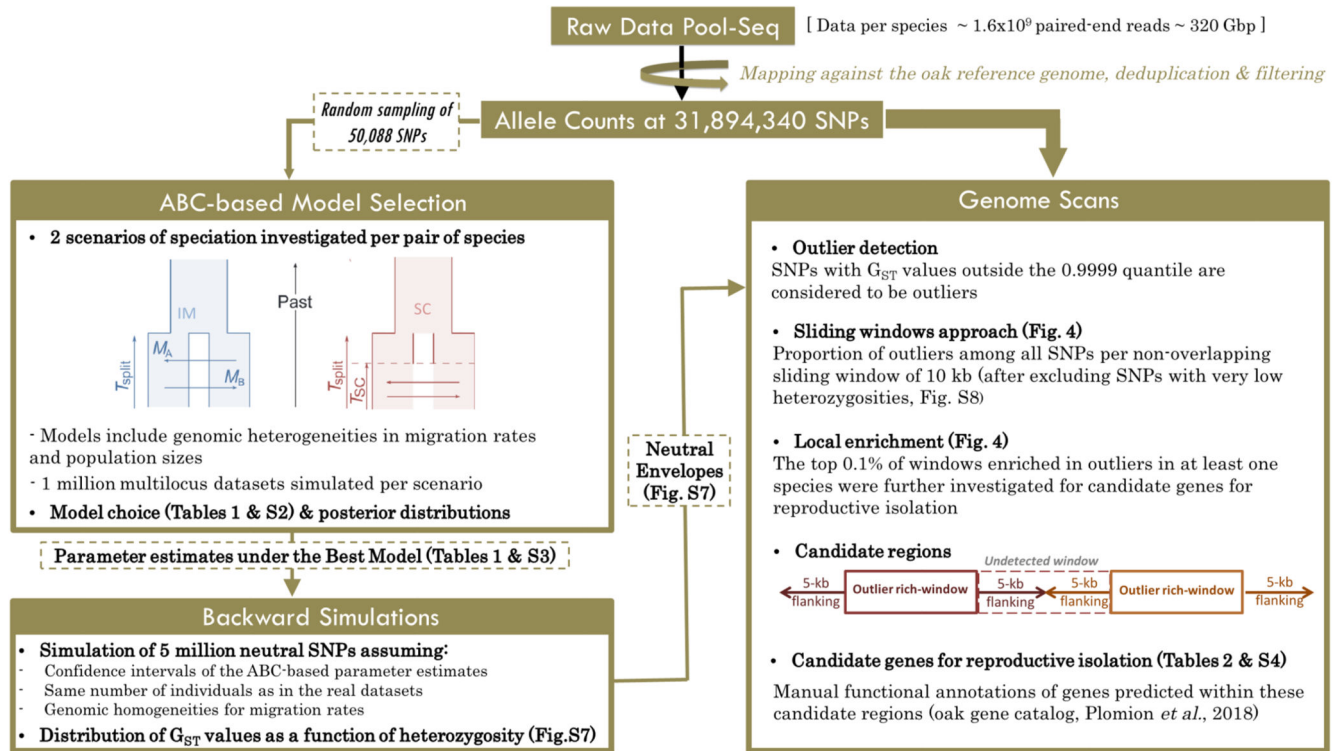
Fig. 2. Workflow used to identify genes contributing to reproductive isolation between four European white oak species.

A subset of 50 thousand of the called SNPs was selected at random and used for model selection under an ABC framework and the generation of parameter estimates under the best model. Large neutral datasets were then simulated to create null envelopes for the identification of SNPs displaying significant departure from expectations under neutrality. We searched for candidate genes in regions enriched in outliers.
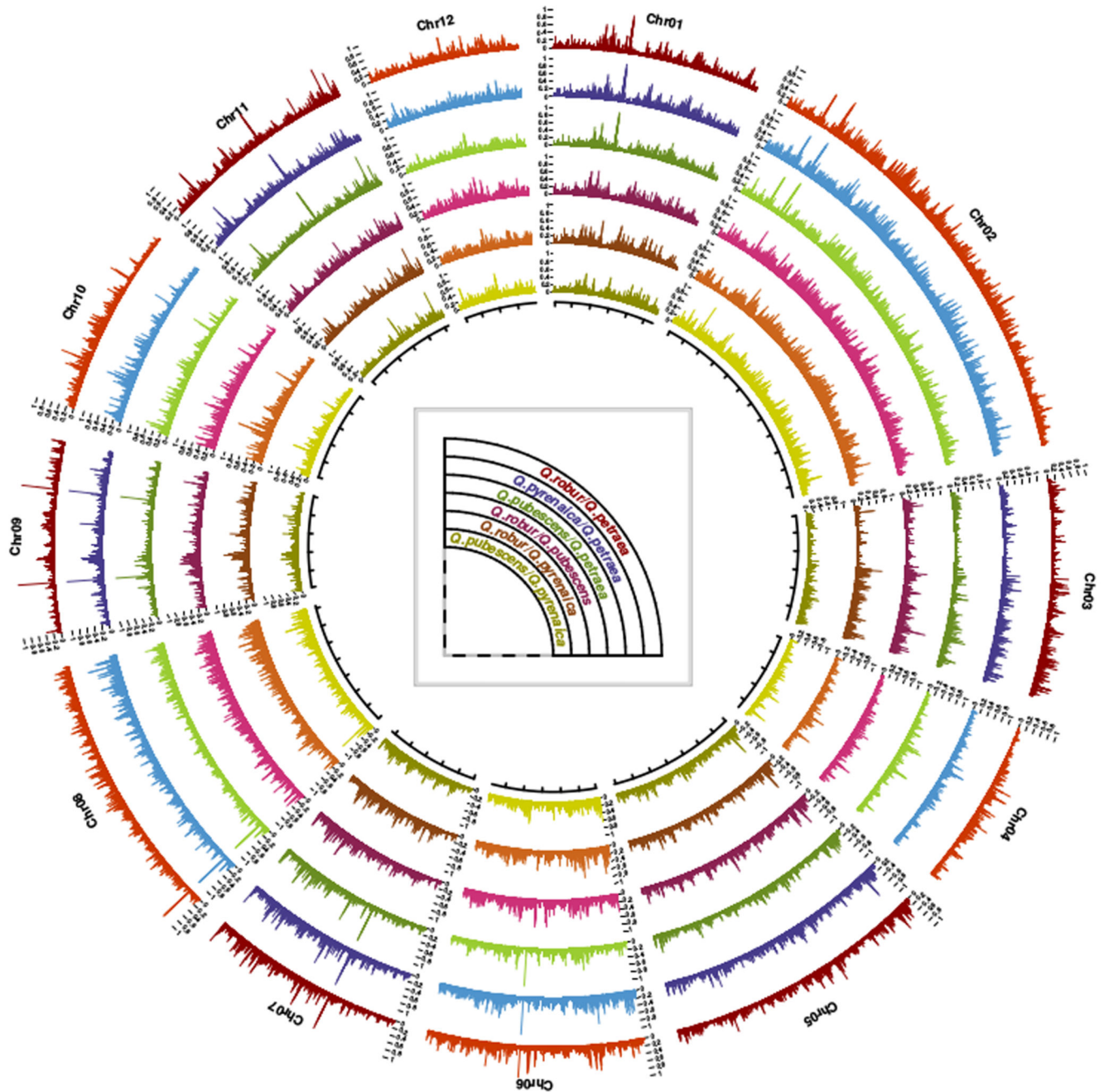
Fig. 3. Circular representation of F_{ST} values along the 12 oak chromosomes.
F_{ST} was calculated from allele frequencies, using non-overlapping 10 kb sliding windows
(detailed patterns are accessible from: https://github.com/ThibaultLeroyFr/
GenomeScansByABC/).
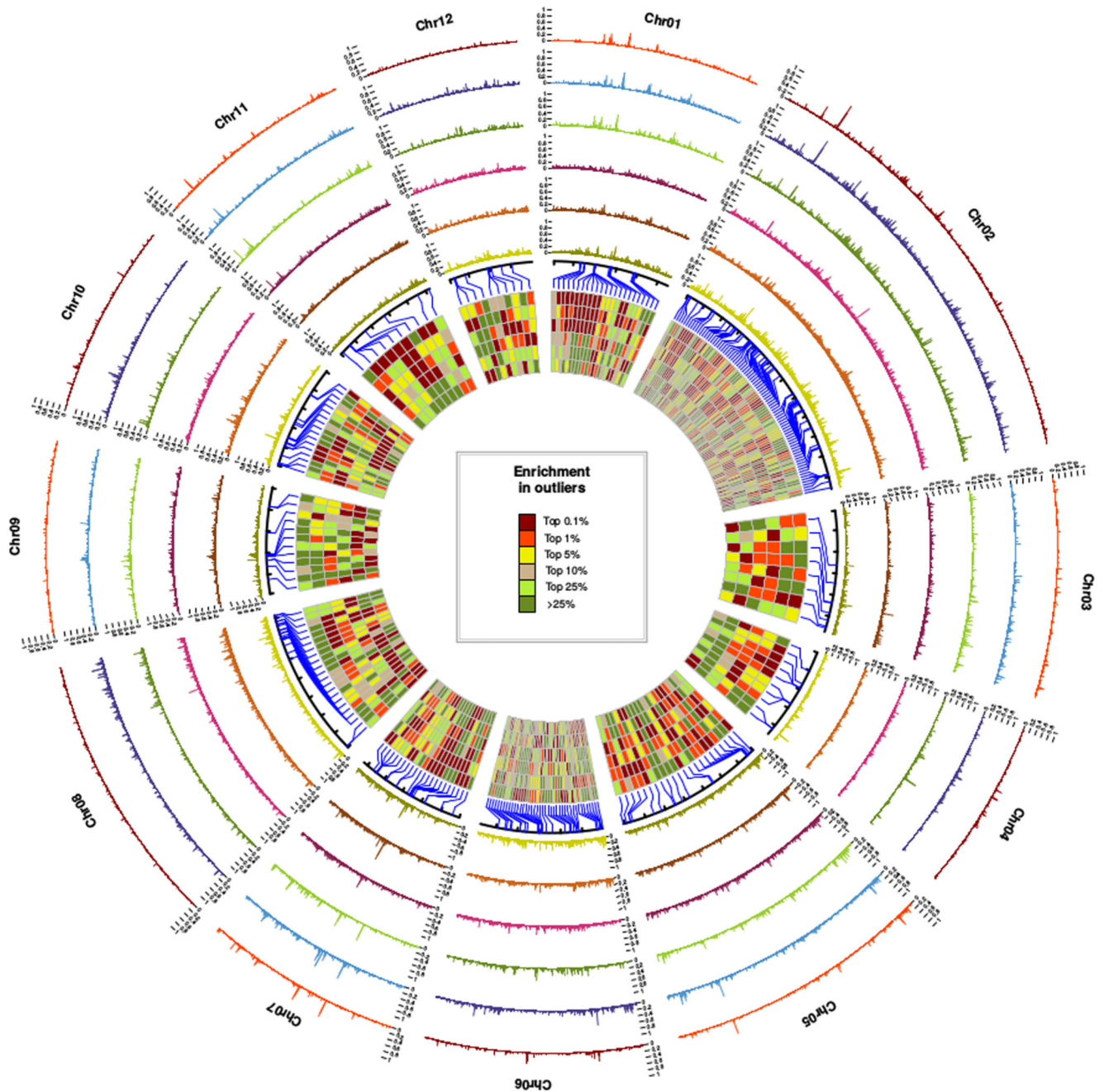
Fig. 4. Local density in outliers per non-overlapping 10 kb sliding window.
From outside to inside, the species pairs are *Q. robur/Q. petraea, Q. pyrenaica/Q. petraea, Q. pubescens/Q. petraea, Q. robur/Q. pubescens, Q. robur/Q. pyrenaica* and *Q. pubescens/Q. pyrenaica*. An outlier corresponds to a SNP with a level of differentiation exceeding the expectations assuming the inferred evolutionary history (0.9999 quantile, see Fig.2 for details). Detailed patterns are accessible from: https://github.com/ThibaultLeroyFr/GenomeScansByABC/. Each rectangle in the inner circle represents the level of enrichment in outliers with He 0.2 for each pair of species at a given position in the genome, assuming

the same order of pairs. These rectangles correspond to the 281 most outlier-enriched windows found in at least one of the six pairs (top 0.1%).

Table 1

Posterior probabilities of the SC scenario and timing of secondary contacts.

Mean (bold) relative posterior probability of the secondary contact scenario and standard deviation (round brackets). Median (bold) and 95% confidence intervals (square brackets) for both the inferred ratio between divergence time (T_{SPLIT}) and time of the secondary contact (T_{SC}) and the secondary contact 'expressed in number of years) after setting T_{SPLIT} to 10 million years (the upper bound for the divergence of this species complex, Hipp et al. 2018). More details are given in Tables S2 & S3.

Pair	Post. Probability SC	T_{SC}/T_{SPLIT} estimates	T_{SC} (years ago)
Q. robur – Q. petraea	**0.98883** (±0.01089)	**1.487 x 10⁻³** [0.43-4.05] x 10⁻³	**14,870** [4,300-40,500]
Q. robur – Q. pyrenaica	**0.99249** (±0.01152)	**1.197 x 10⁻³** [0.31-4.95} x 10⁻³	**11,970** [3,100-40,500]
Q. robur – Q. pubescens	**0.98719** (±0.01342)	**0.245 x 10⁻³** [0.09-0.72} x 10⁻³	**2,450** [900-7,200]
Q. pubescens – Q. petraea	**0.98549** (±0.02231)	**2.176 x 10⁻³** [0.77-6.24] x 10⁻³	**21,760** [7,700-62,400]
Q. pubescens – Q. pyrenaica	**0.99087** (±0.01152)	**0.865 x 10⁻³** [0.32-2.16] x 10⁻³	**8,650** [3,200-21,600]
Q. pyrenaica – Q. petraea	**0.99378** (±0.00697)	**0.383 x 10⁻³** [0.10-1.14] x 10⁻³	**3,830** [1,000-11,400]

Table 2

Genomic positions, gene names, annotations for 32 selected candidate genes for intrinsic and ecological functions driving reproductive isolation.

All other annotations are available in Table S3 (see Dataset S1 for details, including references). Species patterns were determined from the analysis of the most outlier-enriched windows between pairs, as detailed in Table S5.

chr.	positions (regions)	Candidate gene	Gene name	Gene functions	#Paralogs	Pattern
Intrinsic barriers						
Flowering						
Chr08	62493250-62513250	Qrob_P0412860.2	Two-component response regulator-like PRR73	photoperiodic flowering response, circadian clock	1	Complex
Chr08	62673250-62693250	Qrob_P0749650.2	Floral homeotic protein APETALA 2 | Transcr. factor RAP2-7	Delay transition to flowering time, biotic/abiotic stresses	0	Complex
Chr07	44592072-44632072	Qrob_P0088630.2	Transcr. activator DEMETER (DME) / protein ROS1-like	Transcriptional activator required for floral development	1	Complex
Pollen development (Cycloartenol synthases)						
Chr06	28660694-28680694	Qrob_P0684330.2	Cycloartenol synthase 2	Sterol or triterpenoid synthesis, pollen development	13	Complex
Chr06	28690694-28710694	Qrob_P0684400.2	Cycloartenol synthase 2	Sterol or triterpenoid synthesis, pollen development	13	Shared
Chr06	28770694-28810694	Qrob_P0684360.2	Cycloartenol synthase 2	Sterol or triterpenoid synthesis, pollen development	13	Shared
Pollen recognition & seed germination (G-type lectin S-receptor-like Serine/threonine kinase genes)						
Chr03	26118565-26138565	Qrob_P0538230.2	G-type lectin S-receptor-like STK At2g19130	Putatively involved in recognition of pollen	0	Complex
Chr05	4001785-4021785	Qrob_P0641650.2	G-type lectin S-receptor-like STK At1g11300	Putatively involved in recognition of pollen	190	Complex
Chr06	1453464-1473464	Qrob_P0430150.2	G-type lectin S-receptor-like STK LECRK	Regulates expression of immunity genes & seed germination	36	**Q. pyrenaica-specific**
Chr06	1513464-1563464	Qrob_P0430190.2	G-type lectin S-receptor-like STK LECRK	Regulates expression of immunity genes & seed germination	36	**Q. pyrenaica-specific**
Chr08	1749735-1769735	Qrob_P0138480.2	G-type lectin S-receptor-like STK LECRK	Regulates expression of immunity genes & seed germination	36	**Q. pyrenaica-specific**
Embryo development & organogenesis						
Chr12	30514806-30534806	Qrob_P0436820.2	Transcriptional corepressor LEUNIG-like isoform	Leaf, flower (gynoecium) and embryo development	5	**All except. Q. pub/Q.pyr**
Chr02	31611918-31651918	Qrob_P0297580.2	CHD3-type chromatin-remodeling factor PICKLE	Repressor of LEC1, activator of embryo development	0	Complex

chr.	positions (regions)	Candidate gene	Gene name	Gene functions	#Paralogs	Pattern
Chr06	43006752-43026752	Qrob_P0309300.2	Probable N-acetyltransferase HLS1-like	Auxin-responsive gene expression, shoot organogenesis	1	**All except. Q. rob/Q.pet**
Photoreceptor & UV-B tolerance						
Chr08	49805801-49825801	Qrob_P0248780.2	Receptor-like protein 12 (RLP12)	Meristem maintenance control, organogenesis	0	Complex
Chr02	37788250-37808250	Qrob_P0338870.2	Ultraviolet-B receptor UVR8	Photoreceptor/response to UV, circadian clock, stomata	2	Shared
Chr03	34667252-34687252	Qrob_P0500290.2	DNA mismatch repair protein MSH2	UV-B-induced DNA damage response pathway	0	Shared
Chr06	11400887-11420887	Qrob_P0577750.2	Transcription factor MYB12	Positive regulator of flavonoid biosynthesis, UV-B tolerance	0	**All except. Q. rob/Q.pet**
Ecological barriers - abiotic stresses						
Nramp metal transporters						
Chr09	7739510-7759510	Qrob_P0191830.2	Metal transporter Nramp5	Manganese and cadmium uptake	8	**Q. pubescens-specific**
Chr06	38764748-38784748	Qrob_P0097150.2	Metal transporter Nramp6	Involved in iron ion homeostasis	1	**All except. Q. rob/Q.pet**
Dehydration/lateral root growth						
Chr08	68418235-68443235	Qrob_P0457680.2	Protein DEHYDRATION-INDUCED 19-like	Stress-induced sensor, interacting with CPK11 & S-Rnase	0	**All except. Q. rob/Q.pet**
Chr02	27061274-27081274	Qrob_P0304800.2	Transcription factor WER	Controls cell fate specification, e.g. hairy roots or stomata	0	**All except. Q. rob/Q.pet**
Chr02	28240136-28260136	Qrob_P0299670.2	Root Primordium Defective 1 (RPD1)	Lateral root morphogenesis; active cell proliferation	0	Complex
Chr02	36392234-36442234	Qrob_P0422470.2	Alkaline/neutral invertase CINV2	Regulator of root growth, sucrose catabolism	7	Shared
Chr09	19506093-19526093	Qrob_P0418880.2	1-aminocyclopropane-1-carboxylate synthase	Ethylene biosynthetic process, lateral root formation	4	**All except. Q. rob/Q.pet**
Chr04	19182244-19222244	Qrob_P0652510.2	Phosphatidylinositol-3-phosphatase myotubularin-1 (or 2)	Role in soil-water-deficit stress	2	Shared
Chr02	96008743-96028743	Qrob_P0387640.2	Protein WVD2-like 6	Organ stockiness (periph. root cap, trichomes & leafs)	0	**All except. Q. rob/Q.pet**
Freezing/cold adaptation						
Chr09	18556093-18556093	Qrob_P0768740.2	Dehydration-responsive element-binding protein 1	Key role in freezing tolerance and cold acclimation	6	Complex
Chr02	112153196-112173196	Qrob_P0339800.2	B3 domain-containing transcription factor VRN1	Vernalization responsiveness, repressor of FLC	3	**All except. Q. pub/Q.pyr**
Ecological barriers - biotic stresses						
Pathogen resistance/mycorrhization						
Chr10	12310682-12340682	Qrob_P0070130.2	Transportin MOS14	Plant immunity (splicing of resistant genes)	0	**Q. pyrenaica-specific**

chr.	positions (regions)	Candidate gene	Gene name	Gene functions	#Paralogs	Pattern
Chr01	26763631-26783631	Qrob_P0648170.2	Ubiquitin carboxyl-terminal hydrolase 12-like	Protein deubiquitination, regulator of disease resistance	3	Complex
Chr05	3053435-3073435	Qrob_P0622110.2	Nodulation-signaling pathway 1 (NSP1)	Nodulation & mycorrhization	0	Complex